

Efficient and stable field emission from the oxidized porous polysilicon using Pt/Ti multilayer electrode

Seong-Chan Bae · Sie-Young Choi

Received: 13 October 2004 / Accepted: 1 February 2006 / Published online: 1 December 2006
© Springer Science+Business Media, LLC 2006

Abstract The field emission characteristics of an oxidized porous polysilicon (OPPS) were investigated with a Pt/Ti multilayer electrode, which showed highly efficient and stable electron emission characteristics compared with those of conventional Au/NiCr electrodes. The thin Ti layer played an important role in promoting the adhesion of Pt to SiO₂ surface and the distribution of the electric field on the OPPS surface. Additionally, the Ti layer efficiently blocked the diffusion of emitter metal, which resulted in more reliable emission characteristics.

Introduction

Various flat panel displays (FPDs) have been developed to overcome the limitations of conventional cathode ray tube. Recent intensive research has led to the dramatic development and mass production of various FPDs. Field emission displays (FEDs) [1–5] have been also studied intensively with various geometric structures to obtain a clear and wide viewing angle image.

Recently, a new type of field emitter [6–10], an oxidized porous polysilicon (OPPS), has been hailed as the most promising candidate for the field emission display owing to its simple fabrication process and

highly directional electron emission at voltages as low as 10 V. However, the detailed process procedures the OPPS field emitter needs to be investigated to improve its reliability and emission efficiency for application in display devices.

First of all, the thin emitter metals on the OPPS play an important role in the efficiency and stability of field-induced electron emission. The emitter metal should be resistive to external contamination and stable at high temperatures. In addition, the thickness control and the uniform deposition of the emitter metal on the porous surface of the OPPS are crucial for efficient and uniform emission of electrons. The conventional OPPS field emitter [6–11] has adopted Au or its multilayer as a thin emitter electrode due to its low electrical bulk resistivity and resistance to oxidation. However, Au, has a large diffusivity into Si or SiO₂ and is thermally unstable for application to OPPS field emitters.

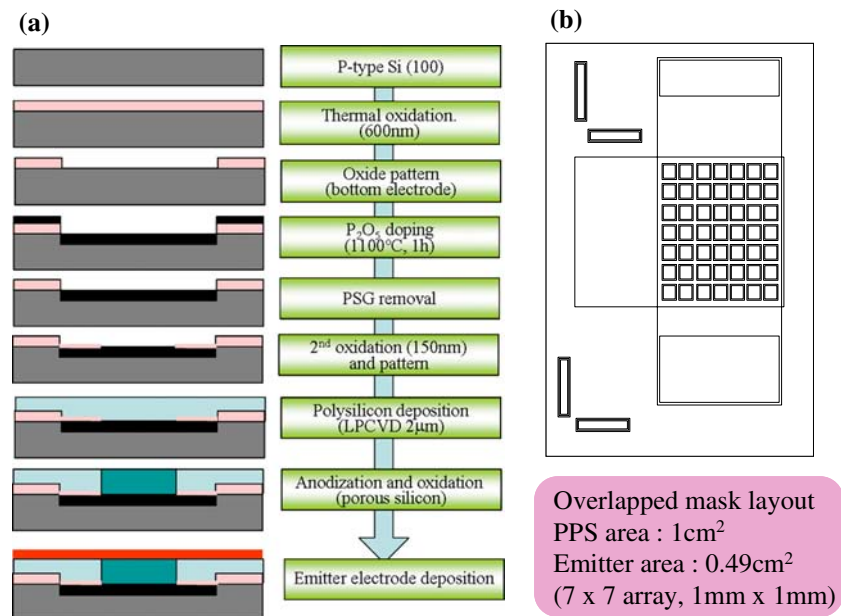
In this study, we chose Pt as an emitter electrode because it is thermally more stable than Au and has good coverage on the porous surface of OPPS. To promote the adhesion of Pt on the OPPS surface, we adopted Ti as an adhesive layer. We investigated the field emission characteristics of OPPS emitters using a Pt/Ti multilayer electrode and compared its field emission properties with those of the Au/NiCr and the Pt electrodes [12]

Experiment

Figure 1 shows the process procedure and mask layout for the fabrication of the OPPS field emitters used in this work. The field oxide was thermally

S.-C. Bae · S.-Y. Choi (✉)
School of Electronic and Electrical Engineering and
Computer Science, Kyungpook National University,
1370 Sankyuk-dong, buk-gu, Daegu 702-701, Korea
e-mail: sychoi@ee.knu.ac.kr

Fig. 1 (a) Fabrication procedure and (b) mask layout of an OPPS field emitter



grown on a p-type (100) Si wafer with a thickness of 600 nm. The field oxide was patterned and P_2O_5 was coated on the patterned Si wafer to define the bottom electrode. After diffusion at 1100 °C for 60 min, the phosphosilicate glass (PSG) was removed, and a second oxide layer was grown and patterned to define the PPS region. Low-pressure chemical-vapor deposition (LPCVD) at 625 °C was used to deposit a polysilicon with a thickness of 1.75 μm . The polysilicon layer was anodized in HF (49%): ethanol = 1:1 solution with a current density of 10 mA/cm^2 for 15 s. The thermal oxidation of the PPS layer was performed for 60 min in a dry O_2 atmosphere with O_2 flow rate of 3 l/min at 900 °C. Three kinds of emitter electrodes, Pt/Ti, Au/NiCr, and Pt electrodes, were deposited using DC sputter and the thickness was controlled with the deposition time. Figure 1b shows the mask layout of the OPPS field emitter. The emission area consists of individual 1 mm \times 1 mm squares which are arranged with 7 \times 7 squares and spaced with 0.5 mm.

Figure 2 shows a schematic cross-sectional view and electrical setup for the investigation of the electrical characteristics of the OPPS field emitter. The electrical characteristics of OPPS field emitters were investigated in a vacuum chamber at a pressure of 2×10^{-5} Torr and with a space of 3 mm between the anode ($V_A = 1$ kV) plate and the OPPS samples. The diode-voltage (V_{ps}) across the OPPS layer was varied from 0 to 20 V, and the emission efficiency ($100 \times I_e/I_{ps}$) was calculated from the ratio of the emission current (I_e) to the diode current (I_{ps} , current flow through the OPPS layer). The

light-emitting pattern was observed on a green phosphor-coated ITO glass plate with a space of 9 mm between the anode plate and the OPPS samples. The anode voltage for observation of the light-emitting pattern was 3 kV. The brightness was measured using a CS-100A brightness meter.

We investigated the field emission characteristics with various Pt/Ti thicknesses and compared the field emission characteristics of Pt/Ti with those of Au/NiCr and Pt emitter electrodes. We also investigated the effects of a relatively thick Al addressing line around the emitter squares and thermal annealing in an N_2 atmosphere on the field emission characteristics of the Pt/Ti OPPS field emitter.

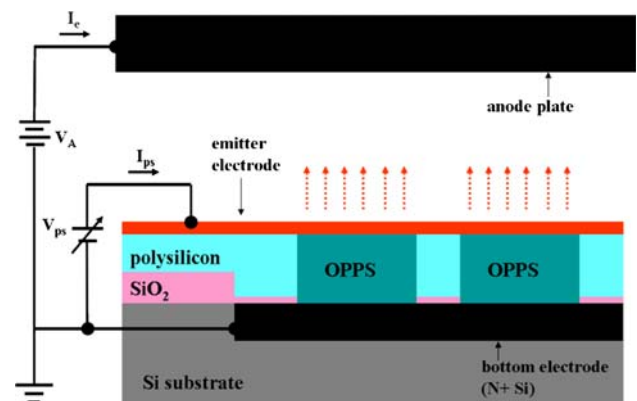


Fig. 2 Schematic diagram of the OPPS field emitter and electrical connection for the investigation of field emission properties

Results and discussion

Formation of oxidized porous polysilicon

Figure 3 shows cross-sectional and surface views of PPS (porous polysilicon) anodized with 10 mA/cm^2 for 15 s. In the cross-sectional view, numerous columnar structured nano-sized pores are apparent on the polysilicon surface and these pores penetrate into the polysilicon layer to a depth of approximately 800 nm. The surface view shows that the pores are dominantly generated in the grain sites because the current mainly flows through the grains. Larger pores are generated at grain boundaries due to large defect density at the grain boundaries. To distribute the applied field over the entire polysilicon layer, we increased the depth of the pore by increasing the anodization time to 40 s, but when we increased the anodization time above 40 s, the PPS layer peeled off at the edge of the PPS region due to penetration of the chemical into the n+ doped bottom electrode.

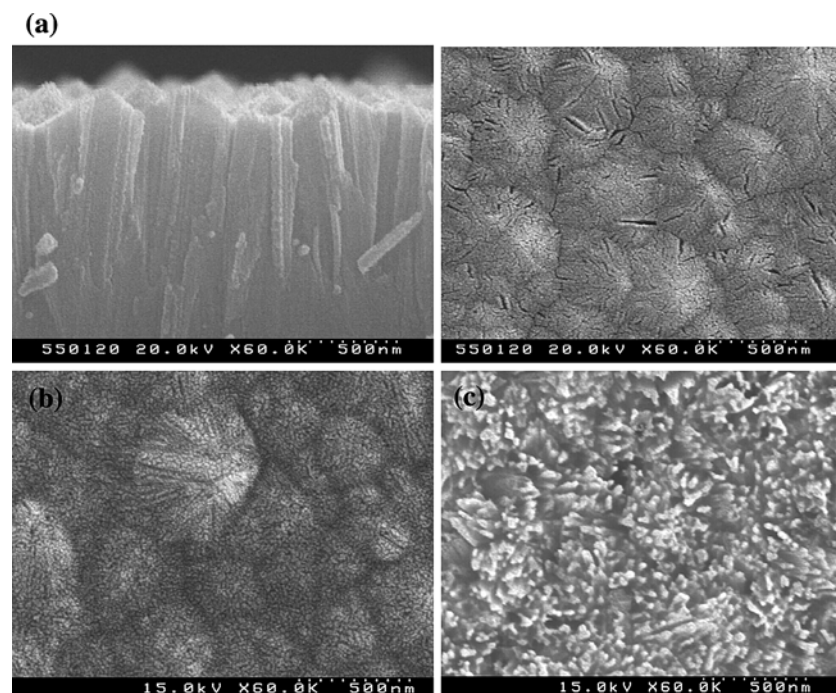
Figure 3b shows the surface of a PPS layer oxidized at the 900°C for 60 min. The oxide thickness on the polysilicon as calibrated by comparison with the thickness on p-type (100) Si was 35 nm for oxidation at $900^\circ\text{C}/60 \text{ min}$. As the oxide grew, the nano-sized pores were filled with oxide which grew from the sides of each pore. Accordingly, the large pores at the surface of the PPS layer gradually disappeared as the oxide grew. In addition, numerous nano-sized pores in

the PPS were filled with oxide and formed a series of oxide/silicon interfaces. To confirm the oxidation behavior of PPS, we etched the oxide of OPPS with BHF for 20 s. Figure 3c shows the surface of the oxide-etched OPPS layer. Oxygen diffused into the porous polysilicon structure, oxidizing the polysilicon to a depth of about 800 nm. The growth of oxide was dominant at the surface of polysilicon and gradually decreased in the polysilicon, which left many silicon tips on the surface of polysilicon after BHF etching as shown in Fig. 3c. Electrons can be emitted by electric field applied to numerous oxidized nano-sized tips and the oxidized silicon nano-crystallite which exists in interstitial site [3].

Field emission characteristics

To fabricate a more stable and efficient OPPS field emitter, we adopted Pt as an emitter electrode. Figure 4a shows the relationship between I_{ps} and I_{e} for Au/NiCr, Pt, and Pt/Ti emitter electrodes. Electron emission in a vacuum starts at a V_{ps} of 7 V and gradually increases with increasing the V_{ps} . The starting point of electron emission coincides with the abrupt increase of I_{ps} , indicating means the tunneling of electrons through the OPPS by applied electric field and the generation of hot electrons which can tunnel the oxide and the thin emitter electrode. The OPPS field emitter which has a Pt/Ti emitter electrode with a thickness of 5 nm/2 nm shows the smallest I_{ps} and I_{e}

Fig. 3 Scanning electron microscopic views of porous and oxidized porous polysilicon, (a) Cross-sectional and surface views of PPS (porous polysilicon) anodized with 10 mA/cm^2 for 15 s, (b) surface view of an oxidized porous polysilicon at 900°C for 60 min, and (c) surface view of porous polysilicon after oxide etch using BHF



below $V_{ps} = 11$ V and the largest I_e above $V_{ps} = 11$ V among three different OPPS field emitters, which results from larger electrical resistance of Pt/Ti multilayer than that of Au/NiCr. Figure 4b shows the emission efficiencies ($100 \times I_e/I_{ps}$) for three different emitter electrodes. Pt/Ti emitter has the highest efficiency, 0.368% at $V_{ps} = 12$ V. Au/NiCr and Pt emitters show less efficient emission characteristics. These results show that Pt/Ti can efficiently apply the electrical field to the OPPS surface and that thin Ti plays an effective role in applying Pt to the electrical field.

The thickness of emitter metal is critical for field emission characteristics of OPPS field emitter. In general, as the thickness of the emitter metal increases, a large portion of tunneled electrons experience scattering in emitter metal, which results in the increase of I_{ps} and less efficient emission characteristic. On the contrary, the electrical field can't be applied to

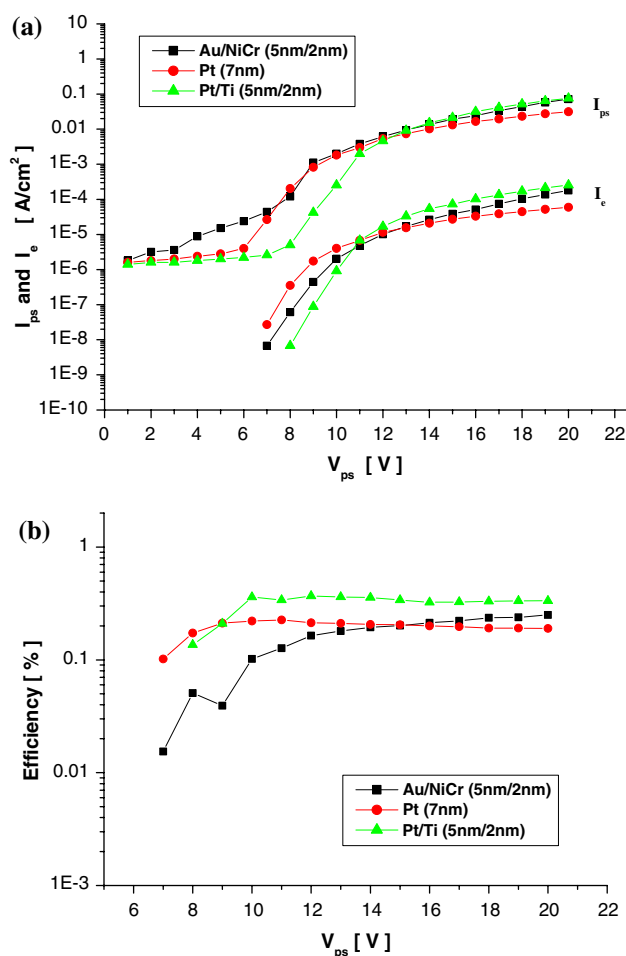


Fig. 4 Field emission characteristics of OPPS field emitters using Pt/Ti, Au/NiCr, and Pt as emitter electrodes, (a) Relationship between I_{ps} and I_e and (b) efficiency

the entire surface of OPPS in the case of too thin emitter electrode. To optimize the Pt/Ti thickness, we investigated the field emission characteristics for different Pt/Ti thicknesses. Figure 5 shows the I_{ps} and I_e characteristics and efficiencies for various Pt/Ti thicknesses. As the thickness of Pt was increased for 2 nm Ti, I_e slightly decreased, but there was no significant considerable change of I_{ps} , I_e , and efficiency. The highest I_e and efficiency (0.656% at $V_{ps} = 10$ V) was observed for Pt/Ti (5 nm/3 nm), and I_e and efficiency abruptly decreased for the Pt thickness of 7.5 nm and 10 nm. These results show that tunneled electrons are abundantly scattered with metal atoms at Pt/Ti thicknesses of above 5 nm/3 nm.

To apply the OPPS field emitter to a display device, the frit or other sealing process is required for the seal

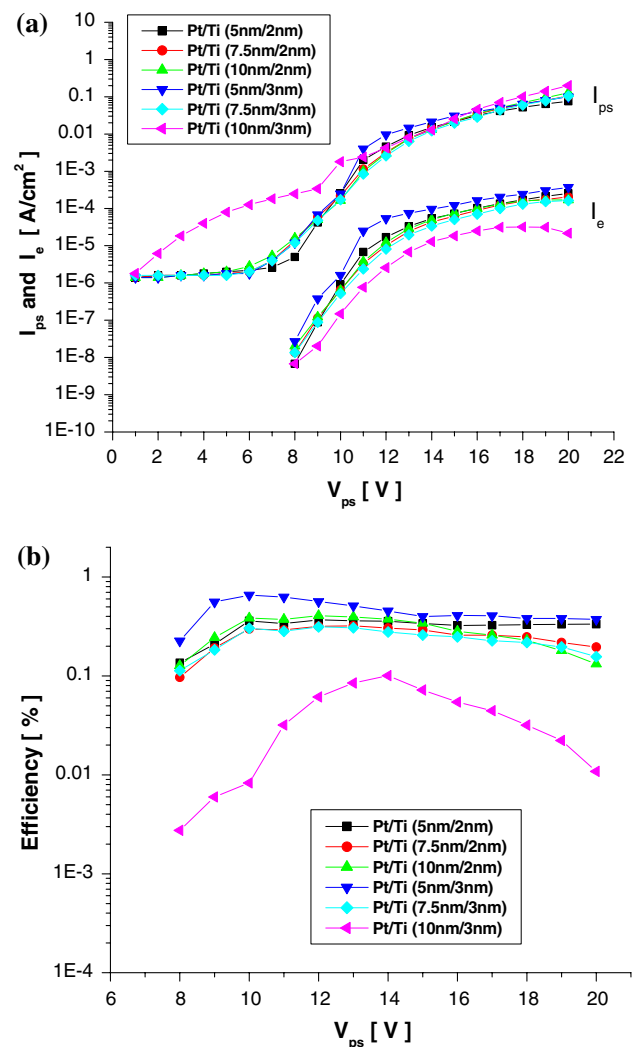


Fig. 5 Field emission characteristics of OPPS field emitters for various Pt/Ti thicknesses, (a) I_{ps} and I_e characteristics and (b) efficiency

emitter device with an anode plate at a temperature range of 300–500 °C in a vacuum atmosphere. Additionally, the adhesion and other performances of the metal electrode can be improved by subsequent thermal annealing. Accordingly, we investigated the effect of thermal annealing in an N₂ atmosphere on the OPPS field emitter which has a sputter-deposited Pt/Ti emitter electrode. Figure 6 shows the effects of thermal annealing on the I_{ps} , I_e , and efficiency of the Pt/Ti OPPS field emitter. Annealing at 300 °C for 1 h significantly increased the I_e and efficiency and a maximum efficiency of 0.7% was observed at $V_{ps} = 12$ V, while annealing at 400 °C for 1 h severely degraded the field emission characteristics. I_{ps} and I_e abruptly decreased due to the diffusion of Pt/Ti emitter metal into the oxide at 400 °C. Diffusion of a thin-emitter metal into oxide caused the failure of inter-connection and electric field application to the OPPS surface. Furthermore, the insulation of oxide broke

down and energetic electrons could not be generated by the electric field.

Thin emitter electrodes can't be used as addressing electrodes by themselves to drive each pixel because a very thin emitter electrode (about 10 nm) has high electrical resistance. Accordingly, a relatively thick metal electrode is required to address each pixel and to minimize the ohmic voltage drop in the thin emitter electrode. In the current study, patterning of Al (150 nm) using evaporation and lift-off was followed by deposition of the Pt/Ti emitter metal. Emitter squares was surrounded by the Al pattern with spacing 100 μm from each corner. Figure 7 shows the field emission characteristics of the Pt/Ti OPPS field emitters which have the as-deposited and the Al-patterned emitter electrode. After the lift-off patterning of Al addressing electrode, the I_e and efficiency are severely degraded, but they are considerably improved after annealing at 300 °C for 1 h. Especially, the efficiency

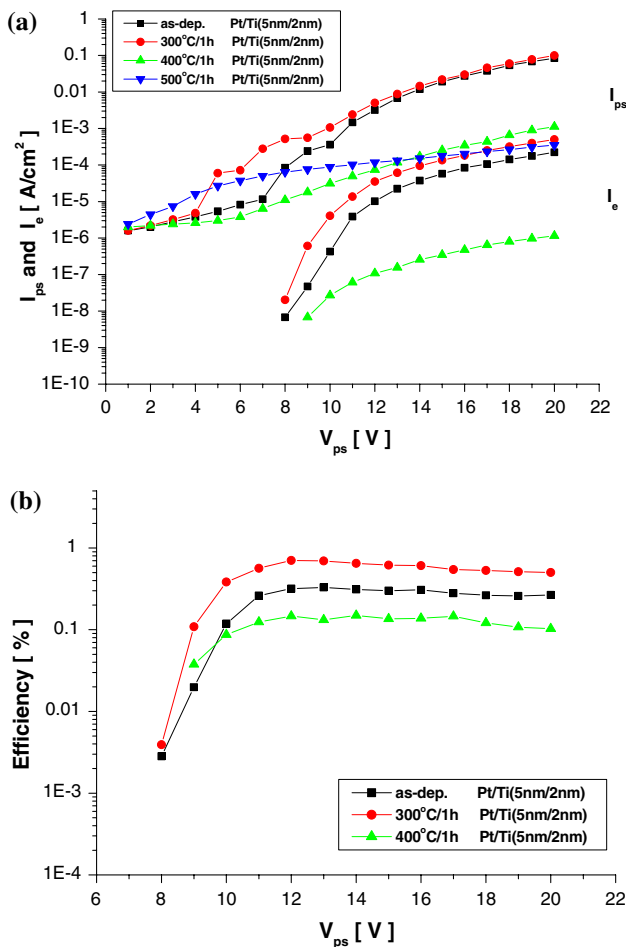


Fig. 6 Effects of thermal annealing on the (a) I_{ps} , I_e , and (b) efficiency of an Pt/Ti OPPS field emitter

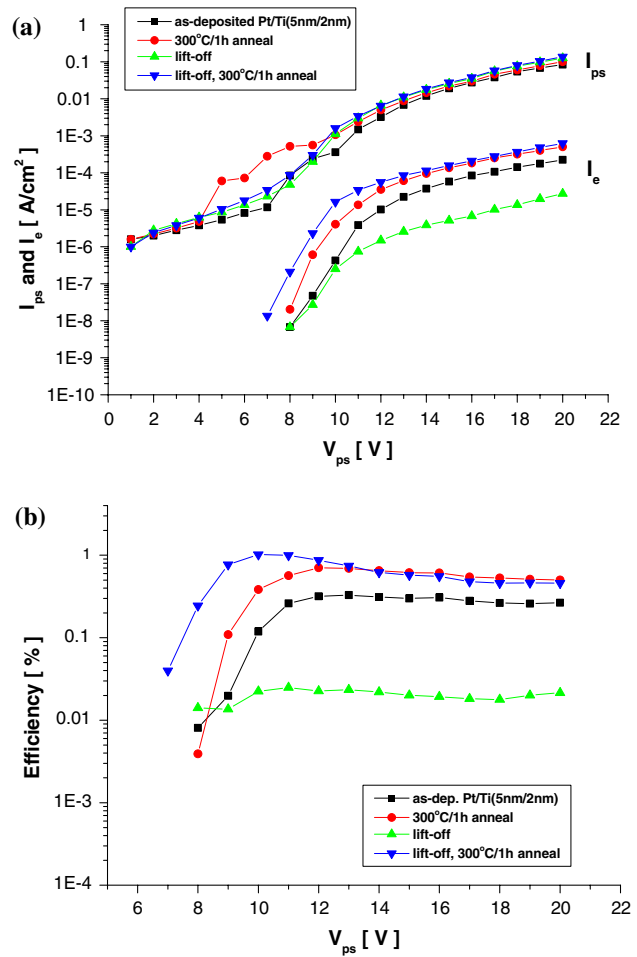


Fig. 7 Field emission characteristics of the Pt/Ti OPPS field emitters which are as-deposited, annealed, patterned using Al, and annealed after Al patterning, (a) I_{ps} and I_e characteristics and (b) efficiency

reaches its maximum value of 1.02% at $V_{ps} = 10$ V. Another notable result is that the electron emission starts at a lower voltage for the Al-patterned and annealed Pt/Ti field emitter. These results show that the Al addressing electrode decreases the voltage drop at the thin emitter electrode and that the electric field is efficiently applied to OPSS emitter region without voltage loss at the thin emitter electrode region. The reason for the improvement of emission characteristics after annealing can be attributed to the adhesion promotion between Al and Pt/Ti metals and the elimination of contaminants which are adsorbed during the lift-off process.

Figure 8 shows the time dependent variation of I_{ps} and I_e at continuous $V_{ps} = 15$ V. For the conventional Au/NiCr OPSS emitter, an abrupt increase and decrease of I_{ps} and I_e are observed, while the Pt/Ti emitter shows more stable field emission behavior. These results show that the thin Ti layer efficiently blocks the diffusion of emitter metal and that the Pt/Ti multilayer is more reliable than Au/NiCr as an emitter electrode for an OPSS field emitter.

To demonstrate the applicability to the display devices, we measured the brightness on a green phosphor-coated ITO glass plate in a vacuum. Figure 9a shows the variation of brightness for the Pt/Ti OPSS field emitter with increasing the V_{ps} . The brightness increases linearly with V_{ps} and reaches 6260 cd/m^2 at a V_{ps} of 20 V and an I_e of 310 $\mu\text{A/cm}^2$. Figure 9b shows the light emission patterns of the Pt/Ti OPSS field emitter. At a distance of 9 mm between the OPSS substrate and phosphor plate, we can observe uniform and clear array of squares, which reveals the vertically directional electron emission of the OPSS

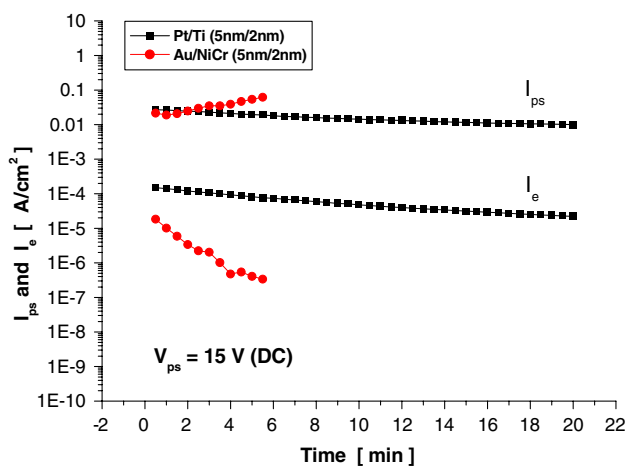


Fig. 8 Reliability measurement for the Pt/Ti and the Au/NiCr OPSS field emitters

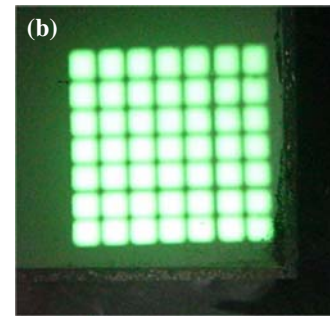
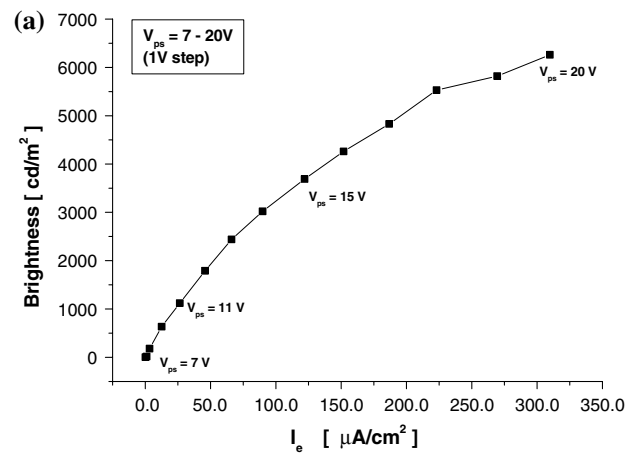


Fig. 9 (a) Variation of brightness for the Pt/Ti OPSS field emitter with increasing the V_{ps} and (b) Emission pattern of the OPSS field emitter on green phosphor at a V_{ps} of 10 V. The emission area consists of 49 squares with each area of 1 mm^2 and I_{ps} and I_e at $V_{ps} = 10$ V are 2.6 mA and 12.5 μA , respectively

field emitter. These results show that the Pt/Ti OPSS emitter is applicable to display devices at a range of $V_{ps} = 10$ –15 V.

Conclusions

To fabricate a more stable and efficient OPSS field emitter, we adopted Pt as an emitter electrode and investigated the emission characteristics of the Pt/Ti OPSS field emitter. The Pt/Ti (5 nm/2 nm) emitter showed a prevailing efficiency of 0.368% at $V_{ps} = 12$ V compared to the Au/NiCr and Pt emitter owing to the thin Ti layer. Annealing at 300 °C for 1 h successfully increased the I_e and efficiency, and a maximum efficiency of 0.7% was observed at $V_{ps} = 12$ V. The Al-addressing electrode and subsequent annealing considerably improved the efficiency, and its maximum value reached 1.02% at $V_{ps} = 10$ V. The Pt/Ti emitter showed more stable field emission behavior than the Au/NiCr emitter in continuous driving conditions because the thin Ti layer efficiently blocks diffusion

of the emitter metal and Pt is thermally more stable than Au/NiCr as an emitter electrode for a OPDS field emitter. The brightness increases linearly with V_{ps} and reaches 6260 cd/m^2 at a V_{ps} of 20 V and an I_e of $310 \mu\text{A/cm}^2$. Accordingly, it is concluded that the Pt/Ti OPDS emitter is applicable for the development of the efficient and stable field emission display devices.

References

1. Spindt CA, Brodie I, Humphrey L, Westerberg ER (1976) *J Appl Phys* 47(12):5248
2. de Heer WA, Chatelain A, Ugarte D (1995) *Science* 270(5239):1179
3. Troyan. PE, Vorobyev GA, Lubsanov RB (1993) *Vacuum Microelectronics Conference*, 124
4. Uemura S, Nagasato T, Yotani J, Kurachi TH, Yamada H (2002) *SID'02 Digest*, 1132
5. Okuda M, Matsutani S, Asai A, Yamano A, Hatanaka K, Hara T, Nakagiri T (1998) *SID Symposium Digest* 29:185
6. Komoda T, Sheng X, Koshida N (1999) *J Vac Sci Technol* 17(3):1076
7. Nakajima Y, Toyama H, Uchida T, Kojima A, Koshida N (2003) *Jpn J Appl Phys* 42:2412
8. Koshida N, Sheng X, Komoda T (1999) *Appl Surf Sci* 146:371
9. Ichihara T, Honda Y, Aizawa K, Komoda T, Nobuyoshi K (2002) *J Cryst Growth* 237–239:1915
10. Lee J-W, Kim H, Ju B-K, Lee Y-H, Jang J (2003) *J Korean Physical Soc* 42:S179
11. Bae S-C, Han S-K, Choi S-Y (2003) *J Korean Physical Soc* 43(6):1053
12. Wolf S, Tauer RN (1986) *Silicon processing VLSI era* 1:250